Pergamon

Adv. Space Res. Vol. 21, No. 4, pp. 637–640, 1998

Printed in Great Britain
0273-1177/98 $19.00 + 0.00

PII: S0273-1177(97)00975-7

LOCAL ION ENERGIZATION AND FIELD STRUCTURE DURING DIPOLARIZATION IN KINETIC AND MHD LIMITS

S. C. Chapman and C. G. Mouikis

Space and Astrophysics Group, Physics Department, University of Warwick, Coventry CV4 7AL, U.K.

ABSTRACT

Self consistent one dimensional hybrid code (particle ions, massless electron fluid) simulations are used to examine the possible structure and evolution of an initially out of equilibrium dipolarizing field reversal in the near earth geotail. Here, we run the simulations in both the ion kinetic (hybrid) limit, where the ion moments and the electromagnetic fields are all well resolved on the scales of the ion motion, and the quasi - MHD limit, where the ion motion is still followed correctly but the ion moments and electromagnetic fields are followed on scales larger than the ion kinetic scales. It is found that the evolution of the magnetic field and ion distribution and hence the pressure tensor are markedly different in the two cases

1. INTRODUCTION

Selfconsistent simulations are now widely used to study magnetospheric boundary layers and structures. Here we address the following question: is it important to self-consistently include in the solution the variations in the bulk plasma moments (number density n, ion current $\mathbf{J}_i$, ion pressure $\underline{\underline{P_i}}$) on ion Larmor scales that arise from the evolving ion distribution?

The example used here is the structure, dynamics and ion energization associated with localized "dipolarization" of flux tubes in the near earth geotail. The initial condition of the simulation is out of equilibrium: the magnetic field reverses smoothly and symmetrically in an isotropic plasma. Subsequently the magnetic reversal relaxes (dipolarizes) as there is insufficient parallel plasma pressure to maintain equilibrium. Hybrid code simulations of this system (Richardson and Chapman, 1994) show that ions are accelerated giving a non isotropic ion pressure tensor which ultimately distorts the magnetic field. A cross tail (GSE y directed) magnetic field component is generated; this B_y component is also seen in hybrid simulations of rotational discontinuities (e.g. Lin and Lee (1993), Cargill et al. (1994)). Particles and waves simply exit the simulation and there is no coupling with an ionosphere, or other external source of plasma. We show results of two self-consistent simulations of this dipolarizing reversal, both of which were obtained using a hybrid code. One is a hybrid simulation in the usual sense; the simulation time step and cell size well resolve the ion Larmor scales. The other is identical except that the cell size has been chosen to be larger than the gyroradii of the ions; hence the trajectories of the individual ions are followed accurately (the time step is still much smaller than the gyroperiod) but the bulk moments are collected onto an MHD scale grid.

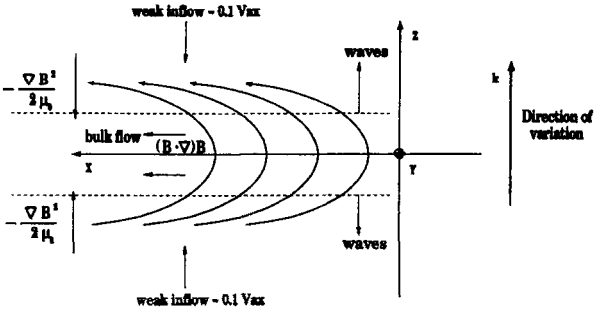

Figure 1: Geometry of the simulation and magnetic field configuration

v_{inflow}	$0.1V_{a,x}$
β_i	0.1
T_e	$0.1\,T_i$
Δz (Hybrid)	$1/10\ R_{gi}$, $0.03\ c/\omega_{pi}$
Δz (MHD scale)	$2\ R_{gi}$, $0.65\ c/\omega_{pi}$
Δt	$1/1630\ \tau_{gi}$
n	$0.2\ cm^{-3}$
B_x	$20nT$
B_z	$2nT$
Grid Points (Hybrid)	4096
Grid Points (MHD)	512
k_{min}, k_{max} (Hybrid)	$0.055, 111.6\ (c/\omega_{pi})^{-1}$
k_{min}, k_{max} (MHD)	$0.019, 4.8\ (c/\omega_{pi})^{-1}$
$\omega_{min}, \omega_{max}$ (both)	$0.1, 800\ (\Omega_{ci})^{-1}$
Particles / Cell	100

Table 1: Parameters for the two simulations

2. SIMULATION DETAILS

The hybrid code scheme used here (Terasawa et al., 1986), (Richardson and Chapman, 1994) represents the ion distribution function with an ensemble of computational particles that follow trajectories prescribed by the Lorentz force law; the change in positions and velocities of these computational particles are resolved on scales that are determined by the time step of the simulation Δt. At each time step the ion number density and current density n_i, $\mathbf{J}_i$ are obtained by taking moments of the computational particle ensemble onto the simulation grid and are hence resolved at the grid spacing Δ_x. The fields are then advanced on the simulation grid using quasineutrality, the "massless" electron fluid momentum equation where the inertial term has been neglected (and with $P_e = nkT_e$, T_e constant), and Maxwell equations at low frequency (displacement current term neglected). At the next time step the fields on the grid are then extrapolated to the particle positions to advance the particle trajectories.

The two simulation runs shown here have identical bulk plasma parameters and time resolution (in terms of the ion Larmor period) differing only in the spatial resolution of the simulation grid. In the hybrid case, $\Delta_x << R_{gi}$ the thermal ion gyroradius in the background field: the fields are advanced using currents resolved on scales $<< R_{gi}$ and the ions experience changes in the fields as they move several Δ_x in a single gyration about the field. In the MHD scale case, $\Delta_x > R_{gi}$: the field advance does not include spatial variations in the current on ion Larmor scales and the ions experience little change in the fields as they remain within a single grid cell Δ_x as they gyrate about the field, only being carried from one cell to the next by field aligned or drift motion of the guiding centre. In both cases the simulation bandwidth (and effect of numerical diffusion due to finite differencing) is such that the expected low frequency modes (see for example Krauss-Varban et al. (1994)) are well resolved (these modes are not identical in the kinetic and the quasi MHD limits). The simulation parameters are summarised in Table 1.

The initial and boundary conditions are identical, the ion distribution is initially isotropic, has weak inflow towards the centre $z = z_0$ and is spatially uniform, $B_x = B_{x0} tanh\left((z - z_0)/L\right)$, $(L = 1.95 c/\omega_{pi})$ $B_y = 0$, the electric field then evolves self-consistently. The boundaries are wave and particle absorbing. The geometry of the one dimensional simulation is shown in Figure 1. All parameters (including all components of the vector and tensor variables) are retained but vary in one space direction ($\hat{z}$) which is directed across the reversal, and time. The field threading the reversal at $t = 0$, B_x, is therefore constant ($\nabla \cdot \mathbf{B} = 0$) in this one dimensional geometry. All waves then propagate in $\pm\hat{z}$.

3. SIMULATION RESULTS

The bulk parameters and ion phase space for the two simulations are shown in Figures 2a (hybrid) and 2b (MHD scale) plotted versus direction of variation across the reversal z. The parameters are shown for $t = 9.8\tau_{gi}$, a time sufficiently late in the simulations corresponding to the "post escape" phase in the hybrid solution (Richardson and Chapman, 1994) when the ions escape from the reversal and can be seen to be moving towards the boundaries.

Electromagnetic Fields

From early times in the simulation, the hybrid solution (which can support field gradients 20 times greater that in the MHD scale situation) is characterised by the growth of a bipolar B_y component as the magnetic field rotates out of the x,z plane across the reversal. The MHD scale solution does not develop significant B_y i.e. the magnetic field remains in the x,z plane. The B_x component is similar in both cases; reversing sharply in a central region where the density is strongly enhanced and being slightly depressed in a region just outside. This depression in B_x just outside the reversal is physically different in the two solutions, however. In the hybrid case, B_x is depressed as the local density is increased by the ions escaping from the reversal. In the MHD scale case, the local density is decreased in this region, accompanied by an increase in the v_z component of bulk velocity into the reversal and an accompanying signature in $E_y = -v_z B_x$. This compressional mode has an analogue in the hybrid solution in the form of a fast mode wave packet which is generated at early times and which has moved out of the simulation box. Other significant differences are the appearance in the hybrid case only of a bipolar signature in the component of $\mathbf{E}$ parallel to the local $\mathbf{B}$ direction, $E_\parallel$ (see Richardson and Chapman (1994)), at the centre of the reversal.

Bulk Plasma Acceleration

The components of $\mathbf{J}\times\mathbf{B}$ are also shown in Figures 2a-2b. In both cases this term is significant only

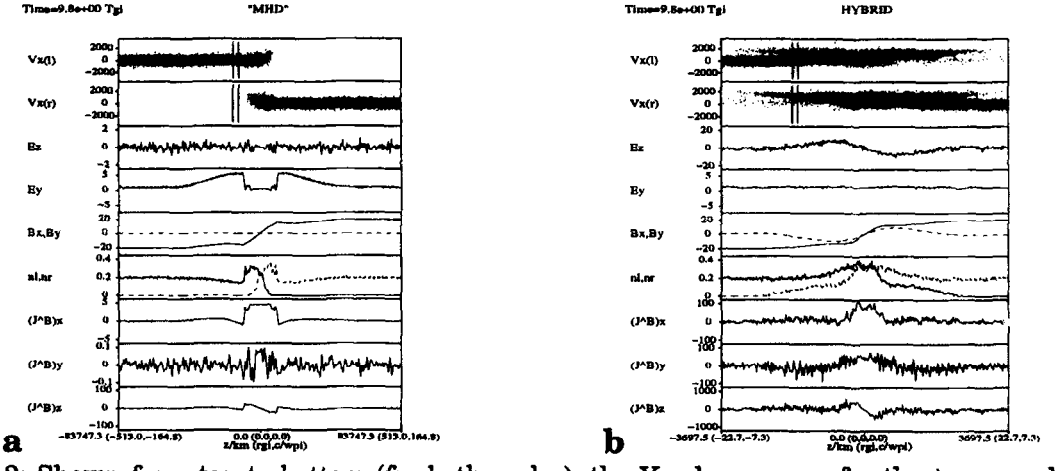

Figure 2: Shown from top to bottom (for both scales): the V_x phase space for the two populations ($km\,s^{-1}$) (the vertical lines indicate regions over which distribution functions will be taken (see Figure 3)), the z and y components of the electric field in ($mV\,m^{-1}$), the magnetic field components B_z (solid), B_y (dashed) (nT), the density of particles of the left-hand (solid) and the right-hand (dashed) populations (cm^{-3}), all three components of the $\mathbf{J}\times\mathbf{B}$ vector.

in the central reversal region so that it does not act on the ions once they have escaped from this region in the hybrid case. The z component then corresponds to ∇B^2 and acts to contain the plasma in the reversal and the x (and in the hybrid case, also y) component corresponds to the curvature force that accelerates the plasma. Although the magnitude of $\mathbf{J}\times\mathbf{B}$ is about 20 times smaller in the MHD scale case, in physical units the width of the central reversal at this time is about 20 times larger, hence the rate of delivery of momentum from the relaxing B field to the plasma over the entire simulation box is the same in both simulations.

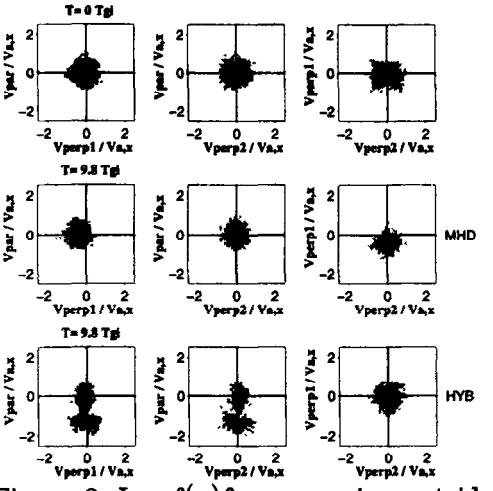

Figure 3: Ion $f(\mathbf{v})$from a region outside the reversal for the MHD scale case and hybrid scale case, the logarithmic grey scale ranges from 1 computational particle per pixel (light grey) to ~50 computational particles per pixel (black).

Ion Distribution Functions

The difference in the ion dynamics in the two cases can be seen in the top panel of Figures 2a and 2b which show v_x of individual computational particles versus z. Distribution functions have been plotted for the regions marked with the vertical lines outside of the reversal (Figure 3). These show projections of the distribution in the $v_\parallel$, $v_{\perp 1}$ plane and the $v_{\perp 1}$, $v_{\perp 2}$ plane. Just outside of the reversal in the MHD scale case the distribution is almost unchanged from the input distribution, it has the same temperature and a cross field drift, in $+z$ (this distribution is taken in the region where there is a significant E_y signature). In the hybrid case the escaping ions can be clearly seen, moving out of the reversal along the field with up to ~ $2v_{a,x}$.

4. CONCLUSIONS

This example indicates that some important features of the hybrid scale solution cannot be ``coarse grained'' to yield the MHD scale solution. The use of the hybrid code to produce an MHD scale solution here has also effectively ensured that the full ion pressure tensor has also been evolved in the MHD scale case. Nonideal representation of MHD, that more fully represent the ion pressure tensor (e.g. Hau (1996)), would not reproduce the hybrid scale solution found here. It should be stressed that the details of these results will differ for different systems, or in more realistic geometry (allowing quantities to vary in three space coordinates). Nevertheless they suggest that variation in ion moments (n, $\mathbf{J}_i$, $\underline{\underline{P}}$) on Larmor scales may need to be self-consistently included in other systems.

This work was conducted whilst C.G.M. was supported by PPARC and S.C.C. was in part supported by a Nuffield Foundation Research Fellowship

5. REFERENCES

1. Cargill, P. J., J. Chen, and J. B. Harold, *Geophys. Res. Lett.*, 21, 2251, 1994
2. Hau, L.-N., *J. Geophys. Res.*, 101, 2655, 1996
3. Krauss-Varban, D., N. Omidi, and K. B. Quest, *J. Geophys. Res.*, 99, 5987, 1994
4. Lin, Y., and L. C. Lee, *J. Geophys. Res.*, 98, 3919, 1993
5. Richardson, A., and S. C. Chapman, *J. Geophys. Res.*, 99, 17391, 1994
6. Terasawa, T., M. Hoshino, J. I. Sakai, and T. Hada, *J. Geophys. Res.*, 91, 4171, 1986